Available online at www.sciencedirect.com

SciVerse ScienceDirect

Proceedings of the Combustion Institute 34 (2013) 2253–2259

Proceedings of the Combustion Institute

www.elsevier.com/locate/proci

Combustion characteristics in a small-scale reactor with catalyst segmentation and cavities

Yueh-Heng Li [a,b,*], Guan-Bang Chen [a], Fang-Hsien Wu [b], Tsarng-Sheng Cheng [c], Yei-Chin Chao [b,*]

[a] Research Center for Energy Technology and Strategy, National Cheng Kung University, Tainan 701, Taiwan, ROC
[b] Department of Aeronautics and Astronautics, National Cheng Kung University, Tainan 701, Taiwan, ROC
[c] Department of Mechanical Engineering, Chung Hua University, Hsinchu 300, Taiwan, ROC

Available online 15 September 2012

Abstract

Hydrogen–air combustion characteristics of a small-scale reactor with different catalyst layouts and configurations are experimentally and numerically investigated. Four different platinum catalyst layouts are used to investigate the effect of catalyst segmentation on combustion performance. It is found that combustion phenomena are strongly related to the variations of inflow velocity, equivalence ratio, and length of catalyst segment. The existence of hetero- and homogeneous reactions in the combustor relies on sufficient catalytically induced exothermicity as well as sufficient hydrogen in the remaining mixture. Besides, the multi-segment catalyst with cavities appreciably extends the stable operating range of catalytic combustion in a small-scale combustor for a wide range of inflow velocities. Nevertheless, gas-phase reaction can be sustained and anchored by the existence of cavity in a small-scale system. The reactor with proposed mechanisms can be applied to various small-scale power, heat generation, and propulsion systems.

Keywords: Catalytic combustion; Catalyst segmentation; Cavity; Small-scale reactor; Hetero- and homogeneous reaction

1. Introduction

Small-scale hydrogen-fueled reactors have been considered as a potential scenario for developing electrical power generation in portable electronics [1–4]. The increased surface-to-volume ratio (S/V) of a small reactor not only increases the heat losses to the wall, but also enhances the possibility of radical termination on the wall. It has been shown that the operating ranges are very narrow for stable combustion in the small-scale combustors [5–8]. Nonetheless, the small-scale catalytic reactors exhibit a wider stability map than that of small-scale homogeneous combustors [9,10]. The catalytic layer deposited on the reactor wall allows sustaining chemical reactions at lower temperatures and higher heat losses, thus reducing the impact of thermal quenching.

In general, the use of small-scale combustor for power system requires high power density, which can be obtained by increasing the inlet mass flow

* Corresponding authors. Address: Research Center for Energy Technology and Strategy, National Cheng Kung University, Tainan 701, Taiwan, ROC. Tel.: +886 6 2757575x31450; fax: + 886-6-238-9940 (Y.-H. Li), Department of Aeronautics and Astronautics, National Cheng Kung University, Tainan 701, Taiwan, ROC. Tel.: +886 6 2757575x63690; fax: +886 6 238 9940 (Y.-C. Chao).
E-mail addresses: yuehheng.li@gmail.com (Y.-H. Li), ycchao@mail.ncku.edu.tw (Y.-C. Chao).

1540-7489/$ - see front matter © 2012 Published by Elsevier Inc. on behalf of The Combustion Institute.
http://dx.doi.org/10.1016/j.proci.2012.06.058

rate and thus gas velocity. On the other hand, to reach high fuel conversions, the residence time must be relatively long which means that low inlet gas velocities are needed to prevent blow-out conditions. As a result, a trade-off in the choice of the inlet gas velocity has to be reached. In order to improve the above shortcomings, novel channel configuration and catalyst layouts [11–16] are proposed to implement in a small-scale reactor. Our previous numerical studies [14–16] indicated that the catalyst segmentation and cavities implemented in a micro-channel can enhance the hetero- and homogeneous reactions and accelerate the fuel conversion in high inflow velocities. Numerical results showed that no significant difference in hydrogen conversion is found among the different catalyst layouts, but the anchoring position of homogeneous reaction in a multi-segment catalyst channel moves upstream as compared to a single catalyst channel. It is no doubt that the effects of heat losses and unknown factors would influence the combustion phenomenon and flammability in a small-scale confined channel. However, numerical simulation is not comprehensively equivalent to complete examination of the combustion phenomena in a small-scale reactor with different catalyst layout and configuration. Therefore, in the present study, the complicated catalytic combustion phenomena in a small-scale reactor with different catalyst layouts and cavities are examined by numerical simulation with detailed chemical and thermal dissipation mechanisms and counter-validated by experimental observations to elucidate the combustion characteristics for the first time.

2. Experimental apparatus

Figure 1 shows the photograph of the small-scale reactor assembly and sketch of experimental apparatus. The reactor has a dimension of 82 mm in length, 20 mm in width and 5 mm in height. A spark igniter and a slot are installed in the reactor. The slot allows placing a ceramic stick coasted with different catalyst layouts and configurations. Two different surfaces, flat and cratered surfaces, of aluminum oxide ceramic stick (60 (l) × 3 (w) × 2 mm (h)) are employed for the present study. For the flat surface, four types of catalyst layouts are considered: eight segments each with 2 mm catalyst, four segments each with 4 mm catalyst, two segments each with 8 mm catalyst, and a 16 mm catalyst without segmentation. The total area of catalyst disposition is kept constant for both with and without catalyst segmentation cases. For the cratered surface, the channel consists of eight segments each with 2 mm catalyst and seven cavities (2 (l) × 3 (w) × 1 mm (d)). The reactor is placed in a digital controlled electrical heater to maintain the surrounding temperature of the chamber at 600 K. A camera is used to record the combustion phenomenon in the channel. Type-R thermocouple is embedded in the exit of the reactor to monitor reaction occurrence, and the correspondingly uncertainty is within ±1%. When the exit temperature is around or below 600 K with dark red color appeared in the channel, it means that only heterogeneous reaction takes place in the reactor. Similarly, when the exit temperature is greater than 1000 K with bright white color anchored in the channel, it means that both hetero- and homogeneous reactions occur in the reactor.

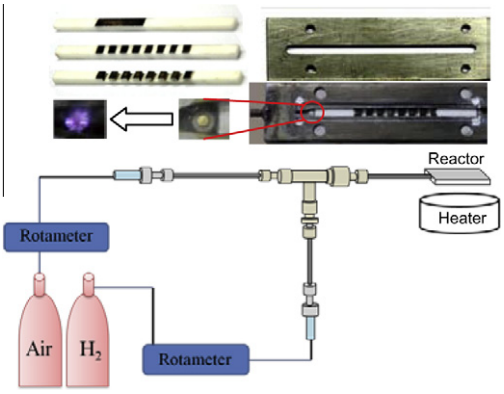

Fig. 1. Photograph of the small-scale reactor assembly and sketch of experimental apparatus.

3. Numerical model and chemical mechanism

A commercial code, CFD-ACE+ [17], is modified to incorporate detailed gas-phase and surface reaction mechanisms in CHEMKIN formats to simulate the flow and reaction characteristics inside the small-scale reactor. For simplicity, the small-scale reactor is modeled as a two-dimensional system with a gap width (L) of 1 mm between the two parallel plates in the numerical simulation. The numerical model consists of steady-state two-dimensional Navier–Stokes equations, mass and energy conservation equations, and species equation for each chemical species. Figure 2 shows the schematic diagram of the

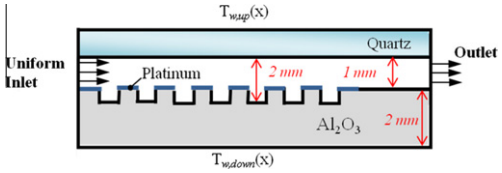

Fig. 2. Schematic diagram of the small-scale reactor model.

small-scale reactor in this work. The computational domain contains both the gas-phase and the surrounding channel walls. The reactor is 65 mm in length and the channel is 1 mm in height. In this work, effects of catalyst segmentation and cavity on fuel reaction enhancement are studied. The concentration of the hydrogen–air mixture is specified at the inlet. The inlet temperature for the fuel/air mixture is 300 K. A uniform velocity profile is specified at the inlet and the flow field is laminar for all cases studied. The thermal boundary condition at the wall is the heat loss to the ambient air. The exterior heat loss includes the heat convection by air and thermal radiation. The exterior wall temperature is specified by experimental data measured by K-type thermocouple and a value of 300 K is specified for ambient air temperature. At the exit, pressure is specified with a constant ambient pressure of 101 kPa.

In the simulations, non-uniform meshes are used with more grids distributed in the reaction region near the wall to provide sufficient grid resolution in the computational domain. The simulation convergence is declared when the residuals of all governing equations approaches steady states. With the convergent criteria, the results reported in this work are achieved with the residuals smaller than 10^{-5}.

Chemical reaction mechanisms are used in the gas phase as well as on the catalyst surface of the inner wall. The homogeneous reaction mechanism of hydrogen–air combustion composes of 9 species and 19 reaction steps; these are adopted from the mechanism proposed by Miller and Bowman [18]. The surface reaction mechanism shown is compiled primarily from that proposed by Deutschmann et al. [19]. These reaction mechanisms have been used in previous studies and the comparisons with experimental results are satisfactory [20–22].

4. Results and discussion

4.1. Effects of catalyst segmentation

In order to understand the effects of catalyst segmentation on combustion characteristics, extensive experiments have been carried out to characterize the reaction performance in the channel with four catalyst layouts. Figure 3 displays the photographs of combustion phenomena in multi-segment catalyst channel with equivalence ratio (ER) of 0.6 and inflow velocity of 20 m/s. This velocity substantially exceeds the flame speed of hydrogen, and thus the homogeneous reaction cannot be sustained in a small-scale reactor with non-catalytic walls under this condition. For a single catalyst with 16 mm-Pt (Fig. 3a), however, the result indicates that only heterogeneous

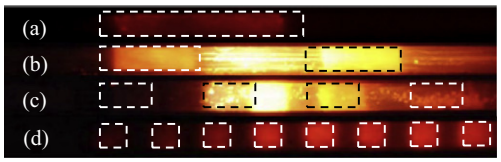

Fig. 3. Photograph of combustion phenomenon for the cases: (a) a 16 mm catalyst without segmentation, (b) two segments each with 8 mm catalyst, (c) four segments each with 4 mm catalyst, and (d) eight segments each with 2 mm catalyst with ER = 0.6 and $V = 20$ m/s.

reaction is observed in the channel. In general, hydrogen has inherently larger mass diffusivity than that of hydrocarbon fuels, and also has relatively high sticking coefficient to platinum catalyst. It is prone to trigger a heterogeneous reaction over catalytic surface even in high inflow velocity. Nevertheless, the conventional competition of fuel and oxidizer on the catalyst bed leads to the inhibition of gaseous reactions. Furthermore, the lack of sufficient heat and fuel concentration in the upstream residual gas could not sustain a homogeneous reaction behind the catalyst. For the cases of two segments each with 8 mm-Pt and four segments each with 4 mm-Pt, both hetero- and homogeneous reactions are observed in the channel. A dim red/orange color at the first catalyst bed and bright white color at the location between adjacent catalyst segments are found in Fig. 3b and c. It appears that hydrogen inherently triggers heterogeneous reaction at the first catalyst section, and then successively induces gas-phase reaction behind the catalyst. The gas-phase reaction is sustained in the non-catalytic walls adjacent to catalyst segments, where the gas inherits prior catalytically induced exothermicity and intermediate radicals. For the case of eight segments with 2 mm-Pt, nonetheless, there is only heterogeneous reaction. It conjectures that the upstream catalyst does not provide sufficient catalyst bed to produce catalytically induced exothermicity for supporting the downstream homogeneous reaction, especially in high flow velocity condition. Accordingly, a sufficient length of catalyst segment is a pivotal parameter to initiate the heterogeneous reaction in the upstream and release sufficient thermal energy to sustain homogeneous reaction in the downstream for preventing thermal and radical quenching on the non-catalytic wall.

Figure 4 shows the experimental observations and numerical simulations of H_2 and OH mass fractions for the reactor that has eight segments each with 2 mm-Pt. The equivalence ratio (ER) of the mixture is 0.6 and the inflow velocity is 20 m/s. Numerical results display certain hydrogen consumption close to the catalyst surface as shown in Fig. 4b, and few OH radical appears in the vicinity of non-catalytic wall adjacent to

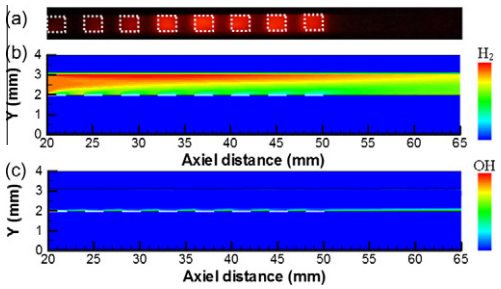

Fig. 4. Experimental observations and numerical simulations of H_2 and OH mass fractions for the reactor with 2 mm-Pt × 8 segments under the condition of ER = 0.6 and $V = 20$ m/s.

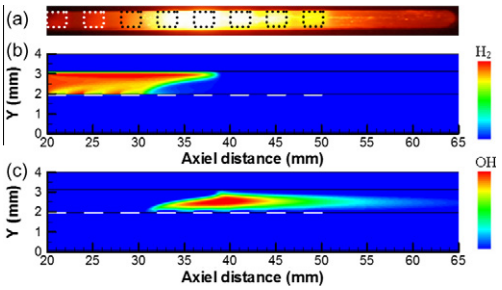

Fig. 6. Experimental observations and numerical simulations of H_2 and OH mass fractions in the reactor with 2 mm-Pt × 8 segments under the condition of ER = 0.8 and $V = 20$ m/s.

catalyst segments as seen in Fig. 4c. It manifests that no homogeneous reaction occurs in the channel, but only heterogeneous reaction. The combustion behavior obtained from numerical simulation is similar to the experimental observation. In order to further examine the reaction behavior in the channel, Fig. 5 shows the computed ratio of surface mass fraction to mean bulk mass fraction along the channel. In general, the heterogeneous reaction can be considered as kinetically controlled, for which the surface concentration is greater than 95% of the bulk concentration. For mass transfer controlled, the surface concentration is less than 5% of the bulk concentration. Figure 5 indicates that hydrogen is consumed periodically on the catalytic surface in the region of the catalyst segments, but the length of catalyst is not long enough to develop into mass-transfer-control region. Some bumps in fuel concentration distributions appear in non-catalytic section, where fuel has no heterogeneous consumption but concentration accumulates due to diffusion from main stream. This explains why hydrogen tends to induce surface reaction over the platinum catalyst, but no gas-phase reaction occurs at the location between adjacent catalyst segments.

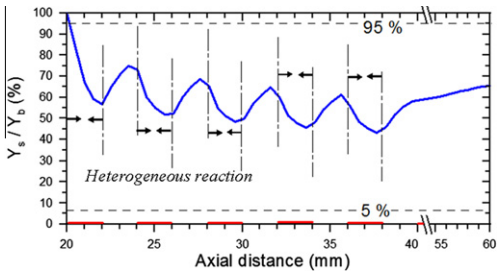

Fig. 5. Computed ratio of surface mass fraction to mean bulk mass fraction of reactant along the channel with 2 mm-Pt × 8 segments under the condition of ER = 0.6 and $V = 20$ m/s.

When the equivalence ratio (ER) of mixture is increased to 0.8 and the inflow velocity is kept at 20 m/s, experimental observations and numerical simulations of H_2 and OH mass fractions for the reactor with eight segments each with 2 mm-Pt are shown in Fig. 6. It can be seen from Fig. 6a that both hetero- and homogeneous reactions occur in this case, but flash-back occurs in the other cases. Although an increase in hydrogen concentration contributes to enhancing hetero- and homogeneous reactions, the increase of flame and wall temperature could result in flame flash-back. Obviously, heterogeneous reaction is initially induced in the upstream catalyst segments, and then gas-phase reaction is anchored at the location between third and fourth catalyst segments and dragged out a flame. Figure 6b exhibits that hydrogen is significantly consumed in the vicinity of upstream catalyst segment due to induced heterogeneous reaction and fuel conversion is completed behind the fourth catalyst segment. The OH mass fraction shown in Fig. 6c reveals that the induced homogeneous reaction behind the third catalyst segment accelerates hydrogen conversion. Figure 6 indicates that the location of homogeneous reaction observed from experiments is in good agreement with numerical predictions. Figure 7 further interprets that the heterogeneous reaction takes place in the upstream catalyst segments, while the downstream catalyst segment inherits thermal energy and thus induces catalytically supported homogeneous combustion. Consequently, the upstream catalyst segments are responsible for initiating surface reaction, while the downstream catalyst segments and spaces are functional to maintain catalytically supported homogeneous combustion.

Figure 8 shows the range of combustion characteristics for four different catalyst layouts with various inflow velocities and ER = 0.6 and 0.8. For ER = 0.6 as shown in Fig. 8a, there is a wider range for hetero- and homogeneous reactions in the case of four catalyst segments each with 4 mm-Pt. This configuration is better than the

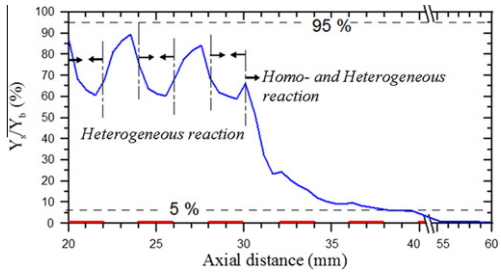

Fig. 7. Computed ratio of surface mass fraction to mean bulk mass fraction of reactant along the channel with 2 mm-Pt × 8 segments under the condition of ER = 0.8 and $V = 20$ m/s.

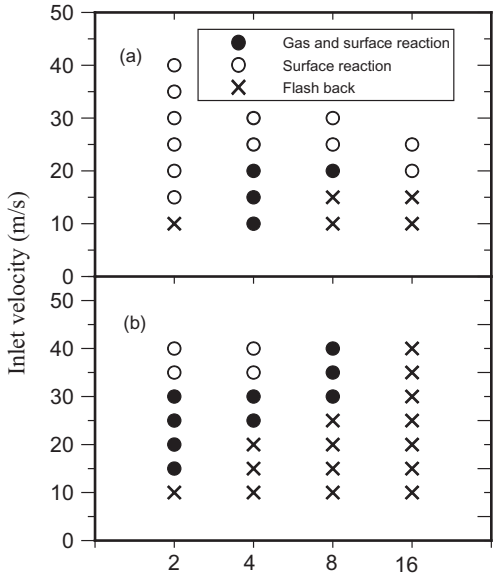

Fig. 8. Operating range of four catalyst layouts with various inflow velocities for (a) ER = 0.6 and (b) ER = 0.8.

other cases. On the contrary, for ER = 0.8 as shown in Fig. 8b, the range for hetero- and homogeneous reactions become wider in the case of eight segments each with 2 mm-Pt, but it is narrower in the cases of four segments with 4 mm-Pt and two segments with 8 mm-Pt. Because of large mass diffusivity and high sticking coefficient of hydrogen, a large amount of hydrogen would inherently deliver to catalyst bed and induce catalytic reaction accompanied with great exothermicity. Therefore, the case with relatively large catalyst segment is prone to have flame flash-back in relative low inflow velocity. Figure 9 shows the combustion phenomena in the reactor for the case of eight segments each with 2 mm-Pt with various inflow velocities ranging from 15 to 40 m/s. Flame anchoring position recedes from the upstream

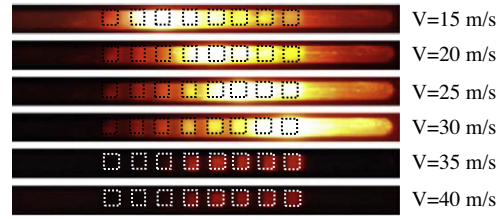

Fig. 9. Photograph of combustion phenomenon in the catalytic reactor (2 mm-Pt × 8 segments) with various inflow velocities.

segment to the downstream segment as the inflow velocity is increased from 15 to 30 m/s. When the inflow velocity is increased to 35 m/s, gas-phase reaction could not sustain inside the small-scale reactor and only surface reaction exists. Consequently, hydrogen combustion behavior in multi-segment catalyst channel is strongly related to fuel concentration, inflow velocity, and catalyst length, which influence the thermal balance between catalytically induced exothermicity and heat losses to the wall.

4.2. Effects of cavity

In order to improve flame stability in the channel for various inflow velocity and fuel concentration conditions, cavity is implemented in the reactor. Figure 10a shows the experimental observations and numerical simulations of H_2 and OH mass fractions and velocity distribution in the reactor with eight segments each with 2 mm-Pt and cavities under the condition of ER = 0.4 and $V = 20$ m/s. Numerical results display that heterogeneous reaction at the first catalyst

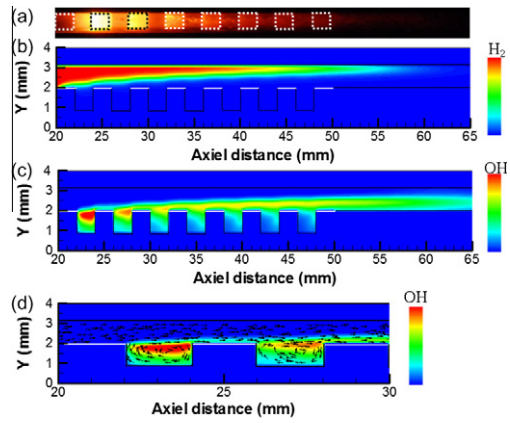

Fig. 10. Experimental observations and numerical simulations of H_2 and OH mass fractions and velocity distribution in the reactor with 2 mm-Pt × 8 segments and cavities under the condition of ER = 0.4 and $V = 20$ m/s.

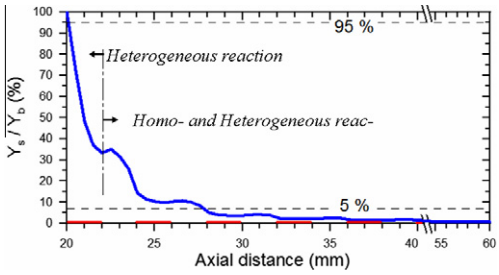

Fig. 11. Computed ratio of surface mass fraction to mean bulk mass fraction of reactant along the channel with 2 mm-Pt × 8 segments and cavities under the condition of ER = 0.4 and $V = 20$ m/s.

segment delivers radicals and heat to the first cavity, and promotes the homogeneous reaction in the cavity, as seen in Fig. 10b and c. Cavities enhance the stabilization of homogeneous reaction by providing a low-velocity asylum, as seen in Fig. 10d. The congregation of OH radicals in the cavities represents flame anchoring, and the calculated flame anchoring location is in good agreement with experimental observation (Fig. 10a). Figure 11 shows that a large amount of hydrogen is consumed in the first 2 mm and the chemical effect is dominated by heterogeneous reaction. The successive hetero- and homogeneous reactions are stabilized in the first cavity, while the remaining hydrogen is rapidly consumed in the following section. The chemical reaction belongs to catalytically supported homogeneous combustion and fuel conversion is completed in a confined distance. Consequently, the existence of cavity not only provides a low-velocity region for flame stabilization, but also supplies thermal energy to heat up the adjacent catalyst segment and to enhance the catalytic combustion.

Figure 12 shows the top view observation of combustion phenomenon in the channel with eight segments each with 2 mm-Pt and cavities. The inflow velocity is ranging from $V = 10$ to $V = 40$ m/s and ER = 0.4. The reaction characteristics in all flow velocity conditions belong to hetero- and homogeneous reactions except for the case of $V = 10$ m/s. This is due to that the heat

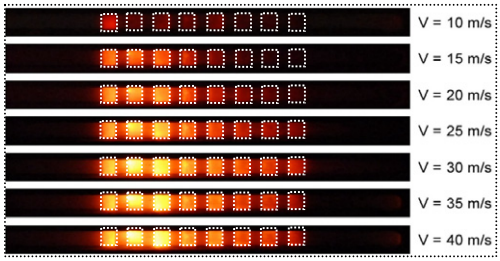

Fig. 12. Photograph of combustion phenomenon in the reactor with eight segments each with 2 mm-Pt and cavities under various inflow velocities.

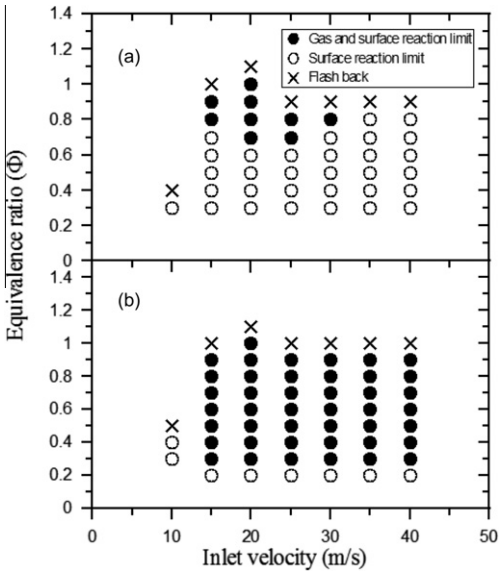

Fig. 13. Operating range of a multi-segment catalyst (a) without and (b) with cavities under various inflow velocities and equivalent ratios.

generation from fuel exothermicity cannot overcome the heat loss from the combustor chamber. It leads to flame quenching on the channel. When hydrogen concentration is increased, homogeneous reaction would appear in the channel. It appears that the flame is anchored at the first cavity for $V \geqslant 15$ m/s. Nevertheless, the unreacted hydrogen could induce homogeneous reaction in the downstream cavities as the inflow velocity is increased. Figure 13 shows the operating range of a multi-segment catalyst with and without cavities under various inflow velocities and equivalent ratios. Owing to physical and chemical characteristics of hydrogen, it is subject to trigger heterogeneous reaction in the upstream catalyst segment and also to induce homogeneous reaction in the upstream cavity. Experimental and numerical results indicate that the existence of cavities appreciably extends the stable operating range of catalytic combustion in the small-scale combustor for a wide range of inflow velocities. Moreover, cavities in a small-scale system can further stabilize the flame and serves as a heat source to enhance the reaction. Consequently, this mechanism resolves the problem of short residence time in high flow velocities and compensates the lack of inadequate heat in low flow velocities.

5. Conclusions

The effects of catalyst segmentation and cavities on enhancement of hydrogen combustion in a small-scale reactor are re-examined by numerical simulation with detailed chemical and thermal

dissipation mechanisms and counter-validated by experimental observations for the first time. These catalyst configurations were considered to improve the hetero- and homogeneous reactions in the reactor. Results reveal that heterogeneous reaction occurred in the prior catalyst segment generates active chemical radicals and catalytically induced exothermicity; a homogeneous reaction is subsequently induced and anchored in the following non-catalytic wall or cavity. Furthermore, the effect of catalyst segment plays an essential role in a catalyst segmentation mechanism, and is strongly related to inflow rate and fuel concentration. Accordingly, flame anchoring position in a multi-segment catalyst channel relied on fluid intensity and fuel concentration. Implementing cavities in a small-scale reactor ameliorates the flame instability and extends the flammability. It is due to that cavities can collect radicals and hot gas from upstream and provide a low-velocity region to sustain and anchor gas-phase reactions.

Acknowledgements

This research was partially supported by the National Science Council of Republic of China under Grant numbers NSC 95-2221-E-006 -392 –MY3 (YCC) and NSC 100-2221-E-216-012-MY2 (TSC). Computer time and numerical packages provided by the National Center for High-Performance Computing, Taiwan (NCHCTaiwan), are gratefully acknowledged.

References

[1] D. Dunn-Rankin, E.M. Leal, D.C. Walther, *Prog. Energy Combust. Sci.* 31 (2005) 422–465.
[2] J. Vican, B.F. Gajdeczko, F.L. Dryer, D.L. Milius, I.A. Aksay, R.A. Yetter, *Proc. Combust. Inst.* 29 (2002) 909–916.
[3] L.C. Chia, B. Feng, *J. Power Sources* 165 (2007) 455–480.
[4] J.A. Federici, E.D. Wetzel, B.R. Geil, D.G. Vlachos, *Proc. Combust. Inst.* 32 (2009) 3011–3018.
[5] S. Raimondeau, D. Norton, D.G. Vlachos, R.I. Masel, *Proc. Combust. Inst.* 29 (2002) 901–907.
[6] D.G. Norton, D.G. Vlachos, *Combust. Flame* 138 (2004) 97–107.
[7] C.M. Spadaccini, A. Mehra, J. Lee, X. Zhang, S. Lukachko, I.A. Waitz, *J. Eng. Gas Turbines Power* 125 (2003) 709–719.
[8] Y.H. Li, Y.C. Chao, N.S. Amadé, D. Dunn-Rankin, *Exp. Therm Fluid Sci.* 32 (2008) 1118–1131.
[9] K. Maruta, K. Takeda, J. Ahn, et al., *Proc. Combust. Inst.* 29 (2002) 957–963.
[10] A. Di Benedetto, V. Di Sarli, G. Russo, *Catal. Today* 147S (2009) S156–S161.
[11] C. Phillips, A. BenRichoub, A. Ambarib, A. Fedorov, *Chem. Eng. Sci.* 58 (2003) 2403–2408.
[12] S. Cimino, L. Lisi, R. Pirone, G. Russo, M. Turco, *Catal. Today* 59 (2000) 19–31.
[13] Y.H. Li, H.W. Hsu, Y.S. Lien, Y.C. Chao, *Int. J. Hydrogen Energy* 34 (2009) 8322–8328.
[14] G.B. Chen, Y.C. Chao, C.P. Chen, *Int. J. Hydrogen Energy* 33 (2008) 2586–2595.
[15] Y.H. Li, G.B. Chen, H.W. Hsu, Y.C. Chao, *Chem. Eng. J.* 160 (2010) 715–722.
[16] Y.H. Li, G.B. Chen, F.H. Wu, T.S. Cheng, Y.C. Chao, *Combust. Flame* 159 (2012) 1644–1651.
[17] CFDRC, CFD-ACE, Huntsville, Alabama, 2003.
[18] J.A. Miller, C.T. Bowman, *Prog. Energy Combust. Sci.* 15 (1989) 287–338.
[19] O. Deutschmann, R. Schmidt, F. Behrendt, J. Warnatz, *Proc. Combust. Inst.* 26 (1996) 1747–1754.
[20] C.P. Chen, Y.C. Chao, Y.C. Wu, J.C. Lee, G.B. Chen, *Combust. Sci. Technol.* 178 (2006) 2039–2060.
[21] O. Deutschmann, L.I. Maier, U. Riedel, A.H. Stroemman, R.W. Dibble, *Catal. Today* 59 (2000) 141–150.
[22] T.S. Cheng, C.Y. Wu, C.P. Chen, Y.H. Li, Y.C. Chao, *Combust. Flame* 146 (2006) 268–282.